Aspects of Higgs Production at the LHC

*Errol Gotsman**

Department of Particles Physics, School of Physics and Astronomy
Raymond and Beverly Sackler Faculty of Exact Science
Tel Aviv University, Tel Aviv 69978, Israel

We discuss the main features and predictions of the GLMM model, which is based on a QCD motivated theoretical approach, and successfully describes the experimental data on total, elastic and diffractive cross sections. In addition we calculate the survival probability for a SM Higgs at the LHC, and compare our results with those of the Durham group.

1 Introduction

Over the past few years the subject of "soft physics" has reemerged from the shadows, and has aroused the interest of the phenomenological community. This in no small way, due to the realization that the calculation of the probability of detecting a diffractive hard pQCD process e.g. Higgs production at the LHC, also depends on the underlying secondaries which are produced by "soft" rescattering. Central diffractive production e.g. (Higgs boson, 2 jets, 2 γ's, χ_c), are accompanied by gaps in rapidity, between the two outgoing projectiles, and the centrally produced particles, which makes their detection easier. The subject of the survival of these rapidity gaps was initiated over twenty years ago [1], and has been refined over the interim period [2, 3].

2 Details of our Model

The details on which our two channel (GLM) model is based i.e. the Good-Walker (G-W) mechanism [4] can be found in [2]. See also U. Maor's talk in these proceedings. It is well known that G-W neglects the diffractive production of large mass states (Mueller diagrams [5]), and to successfully describe the diffractive data, these need to be included by adding the relevant triple Pomeron contributions (see l.h. diagrams in Fig. 1). In addition it is also necessary to include diagrams containing Pomeron loops, as shown in the r.h. diagrams in Fig. 1.

To simplify the problem of summing the Pomeron loop diagrams, we assume that at high energies only the triple Pomeron interaction is essential, this conjecture has been proved in perturbative QCD (see Refs. [6, 7]). Mueller [8] has shown that in the leading log x approximation of pQCD for a large number of colours ($N_c \gg 1$), the correct degrees of freedom are colourless dipoles.

*e-mail: gotsman@post.tau.ac.il

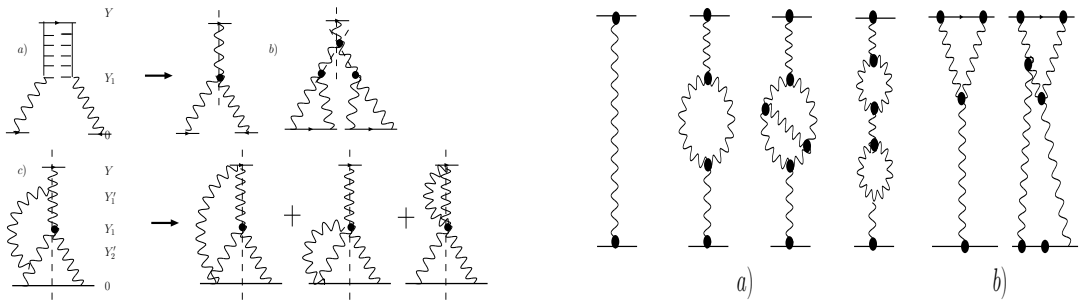

Figure 1: L.h. figure: Examples of Pomeron diagrams not included in G-W mechanism. R.h. figure: Low order terms of the Pomeron Green's function. a) Enhanced. b) Semi-enhanced.

2.1 Summing Interacting Pomeron Diagrams

In the leading order approximation of pQCD, only one Pomeron (dipole) splitting into two Pomerons (dipoles), and two Pomerons (dipoles) merging into one Pomeron (dipole) are considered. All other Pomeron vertices do not appear in the leading log x approximation of pQCD. We therefore restrict ourselves to sum only Pomeron diagrams containing triple Pomeron vertices. We add a caveat, that we neglect the $4I\!P$ term (which is needed for s channel unitarity), however, this term is only significant at energies $W > 10^5$, which is at the limit of the validity of our model.

To make the calculation tractable we further assume that the slope of the Pomeron trajectory $\alpha'_{I\!P} = 0$. The results of our numerical fit to the relevant data, which we will discuss later, ($\alpha'_{I\!P} = 0.01$) lends credence to this assumption.

The theory which includes all the above ingredients can be formulated in terms of a generating function [9, 10]

$$Z(y,\, u) \;=\; \sum_n \; P_n(y)\; u^n, \tag{1}$$

where, $P_n(y)$ is the probability to find n-Pomerons (dipoles) at rapidity y. At rapidity $y = Y = \ln(s/s_0)$ we can impose an arbitrary initial condition. For example, demanding that there is only one fastest parton (dipole), which is $P_1(y = Y) = 1$, while $P_{n>1}(y = Y) = 0$. In this case we have the following initial condition for the generating function

$$Z(y \,=\, Y) \,=\, u\,. \tag{2}$$

At $u = 1$

$$Z(y,\, u \,=\, 1) \;=\; 1, \tag{3}$$

which follows from the physical meaning of P_n as a probability. The solution, with these two conditions, will give us the sum of enhanced diagrams.

For the function $Z\,(u)$ the following simple equation can be written (see Ref. [2] and references therein)

$$-\frac{\partial\, Z(y,\, u)}{\partial\, \mathcal{Y}} \;=\; -\,\Gamma(1 \to 2)\, u\,(1 \,-\, u)\; \frac{\partial\, Z(y,\, u)}{\partial\, u} \;+\; \Gamma(2 \to 1)\, u\,(1 \,-\, u)\; \frac{\partial^2\, Z(y,\, u)}{\partial^2\, u}, \tag{4}$$

where, $\Gamma(1 \to 2)$ describes the decay of one Pomeron (dipole) into two Pomerons (dipoles), while $\Gamma(2 \to 1)$ relates to the merging of two Pomerons (dipoles) into one Pomeron (dipole).

Using the functional Z, we calculate the scattering amplitude [10, 11], using the following formula:

$$N\left(Y\right) \;\equiv\; \mathrm{Im}A_{el}\left(Y\right) \;=\; \sum_{n=1}^{\infty} \frac{(-1)^n}{n!} \;\; \frac{\partial^n Z(y,\, u)}{\partial^n u}\bigg|_{u=1} \gamma_n(Y = Y_0, b), \tag{5}$$

where, $\gamma_n(Y = Y_0, b)$ is the scattering amplitude of n-partons (dipoles) at low energy.

The generating function approach has the advantage that it can be solved analytically (see Ref. [12]), using the MPSI [13] approximation. The exact expression for the Pomeron Green's function is given by

$$G_{I\!P}\left(Y\right) \;=\; 1 \;-\; \exp\left(\frac{1}{T(Y)}\right) \; \frac{1}{T(Y)} \; \Gamma\left(0, \frac{1}{T(Y)}\right), \tag{6}$$

where $\Gamma\left(0, x\right)$ is the incomplete gamma function, and $T\left(Y\right) \;=\; \gamma\, e^{\Delta_{I\!P}\, Y}$. γ denotes the amplitude of the two dipole interaction at low energy. The MPSI approximation only takes into account the first term of the expression of the enhanced diagrams, neglecting other terms, as they are suppressed as $e^{-\Delta Y}$. Consequently, this approximation is only reliable in the region $Y \leq min[\frac{1}{\gamma}, \frac{1}{\alpha'_{I\!P} m_i^2}]$.

3 Determining the Parameters of the Model and Results of the Fit

The pertinent details of our fit to the experimental data, and our determination of the relevant parameters of the model, needed to describe the soft interactions, are contained in [2]. In this section we only mention the salient features, and results of the fit. Our fit is based on

	$\Delta_{I\!P}$	β	$\alpha'_{I\!P}$ GeV^{-2}	g_1 GeV^{-1}	g_2 GeV^{-1}	m_1 GeV	m_2 GeV	$\chi^2/d.o.f.$
GW	0.120	0.46	0.012	1.27	3.33	0.913	0.98	0.87
GW+$I\!P - enh.$	0.335	0.34	0.010	5.82	239.6	1.54	3.06	1.00

Table 1: Fitted parameters for GLMM GW and GW+$I\!P$-enhanced models.

55 experimental data points, which includes the p-p and $\bar{p}$-p total cross sections, integrated elastic cross sections, integrated single and double diffraction cross sections, and the forward slope of the elastic cross section in the ISR-Tevatron energy range. The model gives a good reproduction of the data, with a $\chi^2/d.o.f. \approx 1$. In addition to the quantities contained in the data base, we obtain a good description of the CDF [14] differential elastic cross sections and the single diffractive mass distribution at $t \;=\; 0.05$ GeV^2. An important advantage of our approach, is that the model provides a very good reproduction of the double diffractive (DD) data points. Other attempts to describe the DD data e.g. (see Refs. [15, 3]), were not successful in reproducing the DD experimental results over the whole energy range.

In Table 1 we list the values of the parameters obtained by a least squares fit to the experimental data, both for the G-W formalism (elastic data only), and for the G-W formalism plus

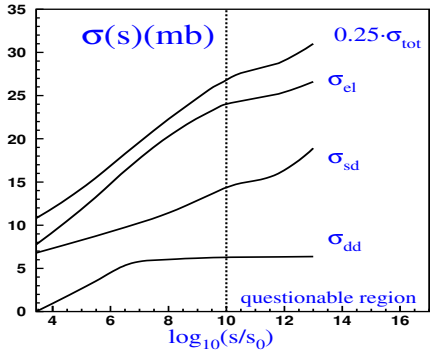

Figure 2: Energy dependence of GLMM cross sections.

enhanced graphs (elastic plus diffractive data). In Table 2 we compare our results with results of the two versions of the model proposed by the Durham group [15, 3]. In Fig. 2 we display the predictions of the GLMM model's values for the various cross sections. Note that σ_{el} and σ_{sd} have completely different energy dependence, unlike the predictions of [3]. At an energy of 7 TeV the predictions of GLMM are (in mb): σ_{tot}= 86.0, σ_{el}= 19.5, σ_{sd}= 10.7, σ_{dd} = 5.9 and the forward slope $B_{el} = 19.4\,\mathrm{GeV}^{-2}$.

	Tevatron			LHC			W=10^5 GeV		
	GLMM	KMR(07)	KMR(08)	GLMM	KMR(07)	KMR(08)	GLMM	KMR(07)	KMR(08)
σ_{tot}	73.3	74.0	73.7	92.1	88.0	91.7	108.0	98.0	108.0
σ_{el}	16.3	16.3	16.4	20.9	20.1	21.5	24.0	22.9	26.2
σ_{sd}	9.8	10.9	13.8	11.8	13.3	19.0	14.4	15.7	24.2
σ_{dd}	5.4	7.2		6.1	13.4		6.3	17.3	
$\frac{\sigma_{el}+\sigma_{diff}}{\sigma_{tot}}$	0.43	0.46		0.42	0.53		0.41	0.57	

Table 2: Comparison of GLMM, KMR(07) and KMR(08) cross sections in mb.

4 Survival Probability for Central Diffractive Production of the Higgs Boson

A general review of survival probability calculations can be found in [16]. We denote by $\langle |\, S^2 \,| \rangle$ the probability that the Large Rapidity Gap (LRG) survives, and is not filled by secondaries from eikonal and enhanced rescattering effects (see Fig. 3). The expression for the survival probability can be written $\langle |\, S^2_{2ch} \,| \rangle = \frac{N(s)}{D(s)}$ where

$N(s) = \int d^2\,b_1\, d^2\,b_2 \left[\sum_{i,k} < p|i >^2 < p|k >^2 \; A^i_H(s,b_1)\, A^k_H(s,b_2)(1 - A^{i,k}_S\,((s,(\mathbf{b}_1+\mathbf{b}_2)))\right]^2$,

and

$D(s) = \int d^2\,b_1\, d^2\,b_2 \left[\sum_{i,k} < p|i >^2 < p|k >^2 \; A^i_H(s,b_1)\, A^k_H(s,b_2)\right]^2$

$A_S(b,s)$ denotes the "soft" strong amplitude of our model [2]. While for the "hard" amplitude $A_H(b,s)$, we assume an input Gaussian b dependence. i.e. $A^H_{i,k} = A_H(s)\,\Gamma^H_{i,k}(b)$

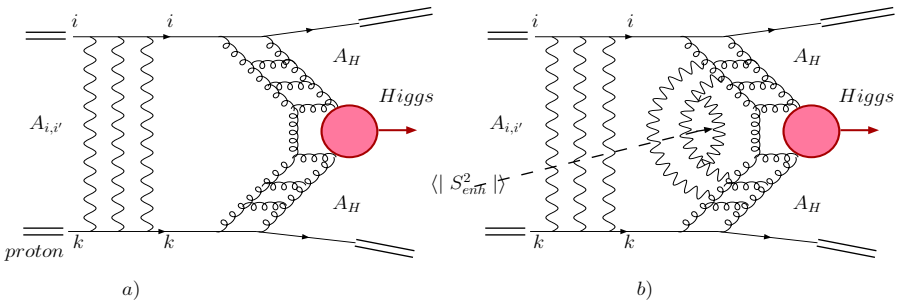

Figure 3: a) the survival probability in the G-W mechanism, b) illustrates the origin of the additional factor $\langle | S^2_{enh} | \rangle$.

with $\Gamma^H_{i,k}(b) = \frac{1}{\pi (R^H_{i,k})^2} e^{-\frac{2b^2}{(R^H_{i,k})^2}}$. The "hard" radii are constants determined from HERA data on elastic and inelastic J/Ψ production. We introduce two hard b-profiles $A^{pp}_H(b) = \frac{V_{p\to p}}{2\pi B^H_{el}} \exp\left(-\frac{b^2}{2\,B^H_{el}}\right)$, and $A^{pdif}_H(b) = \frac{V_{p\to dif}}{2\pi B^H_{in}} \exp\left(-\frac{b^2}{2B^H_{in}}\right)$. The values B^H_{el}=5.0 GeV^{-2} and B^H_{in}=1 GeV^{-2} have been taken from ZEUS data. The value B^H_{el}= (3.6) GeV^{-2} was used in [2], this has now been changed in light of the latest measurements of the "hard" slope, by the H1 group. This is in contrast to KMR treatment [15] where they assume: $A^{pp}_H(b) = A^{pdif}_H(b) \propto \exp\left(-\frac{b^2}{2B^H}\right)$ with $B^H_{el} = B^H_{inel} = 4$ or 5.5 GeV^{-2} The sensitivity of our results to the parameters of the "hard" amplitude are shown in Fig. 4 (left), note that for B^H_{in} =1 GeV^{-2}, changing the value of B^H_{el} from 3.6 to 5.0 GeV^{-2}, increases $\langle | S^2_{2ch} | \rangle$ by $\approx$ 70 % . Our results for $\langle | S^2 | \rangle$ = $\langle | S^2_{2ch} | \rangle$ x $\langle | S^2_{enh} | \rangle$ is given by the full line in Fig. 4 (right), it decreases with increasing energy, due to the behaviour of $\langle | S^2_{enh} | \rangle$.

Our results and the Durham group's results for Survival Probability are given in Table 3. At

	Tevatron			LHC (14 TeV)			W=10^5 GeV		
	GLMM	KMR(07)	KMR(08)	GLMM	KMR(07)	KMR(08)	GLMM	KMR(07)	KMR(08)
S^2_{2ch}(%)	v 5.3		2.7-4.8	3.9	1.2-3.2		3.2		0.9-2.5
S^2_{enh}(%)	28.5		100	6.3	100	33.3	3.3		100
S^2(%)	1.51		2.7-4.8	0.24	1.2-3.2	1.5	0.11		0.9-2.5

Table 3: Comparison of results obtained for Survival Probability in Tel Aviv and Durham models

an energy of 7 TeV we predict a value $\langle | S^2 | \rangle \approx 0.6\%$. We have also succeeded in summing the semi-enhanced contribution (see r.h. side of Fig. 1) to the Survival Probability, and find that it is almost energy independent, and has a value $\approx$ 100% at Tevatron and LHC energies [17].

5 Discussion and Conclusions

We present a model for soft interactions having two components: (i) G-W mechanism for elastic and low mass diffractive scattering, and (ii) Pomeron enhanced contributions for high mass diffractive production. In addition we find from our fit that the slope of the Pomeron

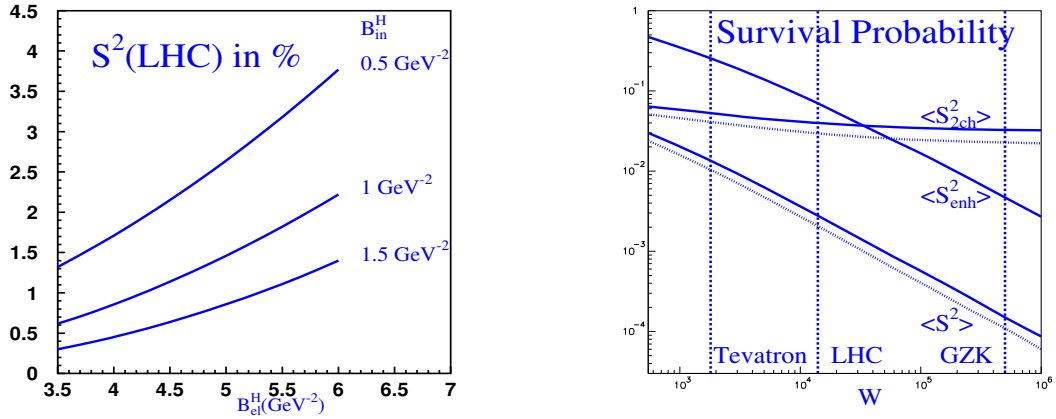

Figure 4: L.h. figure: The dependence of S^2 at the LHC on B^H_{el} and B^H_{in}. R.h. figure: Energy dependence of S^2 for centrally produced Higgs. The full (dashed) line is for $B^H_{el} = 5.0$ $(3.6)\,\mathrm{GeV}^{-2}$.

$\alpha'_{I\!P} \approx 0.01$. This is consistent with what one expects in pQCD, since for a BFKL Pomeron $\alpha'_{I\!P} \propto 1/Q_s^2 \to 0$ as $s \to \infty$. Having $\alpha'_{I\!P} \to 0$, provides a necessary condition that links strong (soft) interactions with the hard interactions described by pQCD. A key hypothesis in our model is that the soft processes are not "soft", but originate from short distances. We have only one Pomeron. There is no requirement for a "soft" and "hard" Pomeron. This is in accord with Hera data for F_2, which is smooth throughout the transition region [18].

To illustrate our achievements and problems, we compare our approach with the work of the Durham group [15, 3]. The main difference in the underlying philosophy of the two groups is that, the Durham approach is based on the parton model where there is only a short range rapidity interaction between partons, while we, due to exchange of gluons in QCD, have a long range rapidity interaction. Both approaches consider $\alpha'_{I\!P}$ as being small. In both programs the Pomeron interaction was taken into account. The difference between the two approaches is that KMR made an *ad hoc* "reasonable" assumption, that the multi-Pomeron vertices have the following form, for the transition of n Pomerons to m Pomerons

$$g^n_m \;=\; n\,m\,\lambda^{n+m-2}\,g_N/2 \;=\; n\,m\,\lambda^{n+m-3}\,g_{3I\!P}/2. \tag{7}$$

No theoretical arguments or theoretical models were offered in support of this assumption, which certainly contradicts the pQCD approach [6, 7]. In spite of these differences, the values obtained for the σ_{tot} and σ_{el} are in surprisingly close agreement (see Table 2). It is only in the latest version of the Durham model [3], which includes three components of the Pomeron, with different transverse momenta of the partons in each component (to mimic BFKL diffusion in k_t), that there are fairly large discrepancies in the diffractive sector i.e. σ_{sd} and σ_{dd}. KMR [3] find that at higher energies σ_{sd} and σ_{el} have comparable values and similar energy dependence, this is not so in our description [2] (see Fig. 2). We note that the results presented by Poghosyan at this conference for σ_{sd} and σ_{dd} [19] agree both in magnitude and energy dependence with those obtained in the GLMM model. There is also disagreement in the result for the calculation of

the Survival Probability. In [3], the Survival Probability is now multiplied by a "renormalizing" factor $(\langle p_t^2 \rangle B)^2$ and referred to as $\langle S^2_{eff} \rangle$. The result for LHC energy is $\langle S^2_{eff} \rangle = 0.015^{+0.01}_{-0.005}$. It is not clear whether there is in addition a factor of $\langle S^2_{enh} \rangle \approx 1/3$, that needs to be incorporated. If affirmative, then the discrepancy between our result and that of the Durham group for $\langle S^2 \rangle$ at Tevatron energies is small, but the discrepancy becomes larger for the LHC energy range, as we predict that $\langle S^2_{enh} \rangle$ decreases as the rapidity between the projectiles increases, while Durham claim little (if any) energy dependence for $\langle S^2_{enh} \rangle$.

Acknowledgements

This research was supported in part by BSF grant # 20004019 and by a grant from Israel Ministry of Science and the Foundation for Basic Research of the Russian Federation.

References

[1] Y.L. Dokshitzer, S.I. Troian and V.A. Khoze, Sov. J. Nucl. Phys. **46** 712 (1987); Y.L. Dokshitzer, V.A. Khoze and T. Sjöstrand, Phys. Lett. **B274** 116 (1992); J.D. Bjorken, Intr. J. Mod. Phys. **A7** 4189 (1992); Phys. Rev. **D47** 101 (1993); E. Gotsman, E. Levin and U. Maor, Phys. Lett. **B309** 199 (1993).

[2] E. Gotsman, E. Levin, U, Maor and J.S. Miller, Eur. Phys. J. **C57** 269 (2008).

[3] M.G. Ryskin, A.D. Martin and V.A. Khoze, Eur. Phys. J. **C60** 249 (2009).

[4] M.L. Good and W.D. Walker, Phys. Rev. **120** 1857 (1960).

[5] A.H. Mueller, Phys. Rev. **D2** 2963 (1970).

[6] J. Bartels, M. Braun and G.P. Vacca, Eur. Phys. J. **C40** 419 (2205); J. Bartels and C. Ewerz, JHEP **9909** 026 (1999); J. Bartels and M. Wusthoff, Z. Phys. **C6** 157 (1995); A.H. Mueller and B. Patel, Nucl. Phys. **B425** 471 (1994); J. Bartels, Z. Phys. **C60** 471 (1993).

[7] M.A. Braun: Phys. Lett. **B632** 297 (2006), Eur. Phys. J. **C16** 337 (2000); Phys. Lett. **B483** 115 (2000); Eur. Phys. J. **C33** 113 (2004); M.A. Braun and G.P. Vacca, Eur. Phys. J. **C6** 147 (1999).

[8] A.H. Mueller, Nucl. Phys. **B415** 373 (1994); **B437** 107 (1995).

[9] A.H. Mueller, Nucl. Phys. **B415** 107 (1995).

[10] E. Levin and M. Lubinsky, Nucl. Phys. **A763** 172 (2005); Phys. Lett. **B607** 131 (2005); Nucl. Phys. **A730** 191 (2004).

[11] Y.V. Kovchegov, Phys. Rev. **D60** 034008 (1999).

[12] M. Kozlov and E. Levin, Nucl. Phys **A779** 142 (2006).

[13] A.H. Mueller and B. Patel, Nucl. Phys. **B425** 471 (1994); A.H. Mueller and G.P. Salam, Nucl. Phys. **B475** 293 (1996); G.P. Salam, Nucl. Phys. **B461** 512 (1996); E. Iancu and A.H. Mueller, Nucl. Phys. **A730** 460 (2004).

[14] CDF Collaboration, Phys. Rev. **D50**, 5535 (1994).

[15] M.G. Ryskin, A.D. Martin and V.A. Khoze, Eur. Phys. J. **C54** 199 (2008).

[16] E. Gotsman, E. Levin, U. Maor, E. Naftali, and A. Prygarin, in :HERA and the LHC- A Workshop on the Implications of HERA for LHC Physics: Proceedings Part A, p. 221 (2005). arXiv:hep-ph-0601012

[17] E. Gotsman, E. Levin and U. Maor (to be published).

[18] H1 Collaboration, arXiv:hep-ex/0904.0929 (2009)

[19] A.B. Kaidalov and M.G. Poghosyan, arXiv:hep-ph/0909.5156